SUBSYSTEM DESIGN AND VALIDATION FOR OPTICAL SENSORS FOR MONITORING ENHANCED GEOTHERMAL SYSTEMS

William Challener, Aaron Knobloch, Mahesh Ajgoankar, Pramod Chamarthy, Hua Xia,
GE Research
One Research Circle
Niskayuna, NY, 12309, U.S.A.
e-mail: challene@ge.com

Roger Jones, Russell Craddock, Li Zhao, and Peter Kinnell
GE Sensing
Fir Tree Lane
Groby, Leicestershire, LE6 0FH, U.K.

Trevor W. MacDougall and Paul Sanders
Qorex, LLC
101 Hammer Mill Road
Rocky Hill, CT, 06067, U.S.A.

ABSTRACT

A multidisciplinary team, consisting of participants from GE, Qorex LLC, AFL Telecommunications and Sandia National Labs, is engaged in a DoE-sponsored program to develop an optical sensor suite for the measurement of distributed temperature and pressure in geothermal wells. Our effort in the first year has been focused on the development and validation of specific sub-systems including both fiber and sensors to show the reliability of the sensing approach for temperatures up to 374 C and pressures of 220 bars in the presence of hydrogen. This paper discusses the overall program scope and presents some initial results from three key tasks, point pressure sensor development, fiber Bragg grating pressure sensor development, and fiber tensile strength testing at elevated temperatures.

FIBER OPTIC SENSING SYSTEM FOR ENHANCED GEOTHERMAL SYSTEMS

Temperature and pressure sensing in enhanced geothermal systems is one of the primary needs at present. The harsh environment of such wells leads to difficulty in designing robust sensors. This current project is aimed at developing a fiber optic system that will combine several different types of measurement systems into a single cable. Fiber is currently being evaluated for use at high temperatures (374 C) and high pressures (220 bars). Both its mechanical strength and resistance to hydrogen darkening effects are key concerns. Fiber which is found to be robust under these conditions will be used to operate a MEMS pressure sensor at the bottom of the geothermal well. Another fiber will be used to interrogate Fiber Bragg grating pressure and temperature sensors distributed along the length of the fiber, and especially near the lower end of the well. A graded index multimode fiber will be used as part of a Raman distributed temperature measurement system (DTS). A single mode step index fiber will be used for Brillouin distributed temperature and strain sensing (DTSS), and another fiber for Rayleigh coherent optical time domain reflectometry (COTDR) for distributed strain measurements. All of these fibers will be bundled into a single cable with appropriate strain relief and corrosion resistance with the objective of making these measurement in wells up to 10 km deep for a lifetime of at least six months with a pressure measurement accuracy of better than 1% and a long term drift of less than 1%.

The program is funded by DOE with cost sharing for a period of two years for a total cost of $2.6M. The first year of the project is aimed at developing the various subsystems. In the second year, the subsystems will be integrated into a cable and down hole testing will be undertaken. GE Global Research and GE Sensing are primarily involved in designing and fabricating the MEMS and FBG pressure sensors. Qorex is testing various commercially available fibers for their suitability in the harsh geothermal environment, and is evaluating commercially available instruments for Raman DTS, Brillouin DTSS and Rayleigh COTDR measurements. Qorex will also design the fiber cable, which will be fabricated by AFL Telecommunications. Down hole fiber cable testing will be supervised by Sandia National Laboratory. In this report, we discuss research efforts related to the

MEMS and FBG sensor development, and the initial fiber testing results related to year 1 project tasks.

MEMS POINT PRESSURE SENSOR

It is desirable to have a highly accurate pressure sensor at the bottom of the geothermal well. We have selected a MEMS pressure sensor because of its high accuracy and general suitability for the geothermal environment. MEMS devices, of course, have been employed in a wide variety of pressure sensors. For pressure measurements in a geothermal well, we have chosen an approach similar to that described in (Andres, 1986). A laser at one wavelength is modulated at the resonant frequency of the MEMS sensor. The heat generated in the resonator by absorption of the laser beam causes the resonator to vibrate. The vibration in turn varies the cavity formed by the resonator and the end of the fiber. The reflected beam from a second continuous laser is thereby modulated at the frequency of the resonator vibration and detected.

A simplified block diagram of our sensor design is shown in Fig. 1. It differs from that described by Andres in that a single fiber is used to deliver both the drive and read laser beams. The cavity is formed from surfaces integral to the sensor and, unlike the previously described sensor, is relatively insensitive to the fiber-to-sensor gap other than for an approximately inverse square drop in signal intensity as the fiber gap is increased, as shown in Fig. 2.
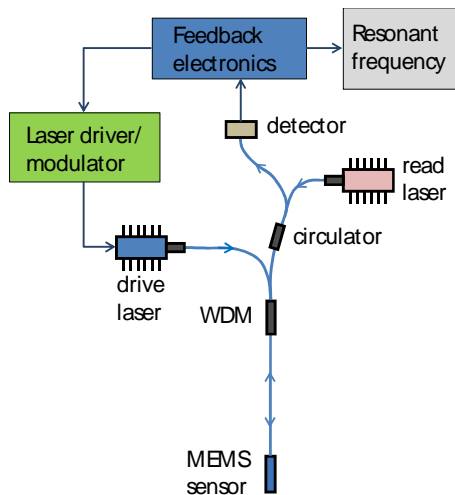

Fig. 1: *Silicon MEMS point pressure sensor that is optically driven and interrogated.*

A priori, there is no reason for the optimum spot on the resonator for the drive laser to be the same as that for the read laser. Extensive finite element analysis has been carried out to determine a resonator design

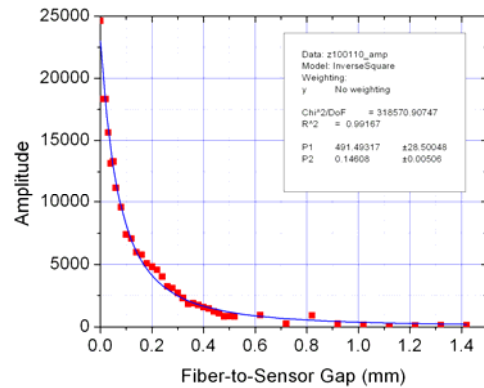that satisfies the constraint of a single fiber to

Fig. 2: *Inverse square decay of signal amplitude as fiber is withdrawn from sensor.*

simplify the sensor package and fiber cable.

With proper alignment of the fiber to the sensor and a resonator that is driven within its linear optical
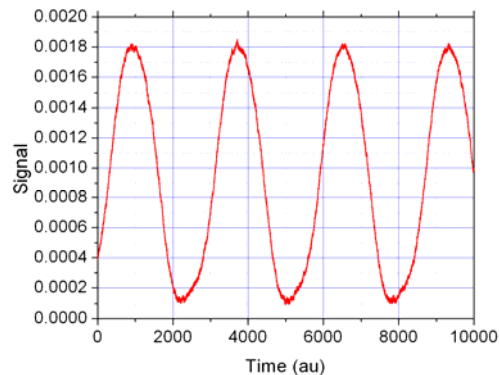

Fig. 3: *Scope capture of the reflected laser intensity modulated by the vibrating resonator demonstrating nearly zero signal amplitude at the minima.*

response range, a reasonably sinusoidal readback signal can be obtained as shown in Fig. 3.

The results in Fig. 3 were obtained at atmospheric pressure for a MEMS sensor optimized for pressures below 2 bars and driven electrically. Sensors have now been designed for this high pressure/high temperature geothermal application and will be tested and calibrated using a complete optical system including a feedback loop as shown in Fig. 1.

Other challenges in the system design that are being addressed include the fiber-to-sensor splice, the fiber-to-sensor package connection, and the sensor package design that enables the well pressure to be conveyed

to the MEMS sensor without exposing the sensor itself to the harsh chemical environment.

DISTRIBUTED FIBER BRAGG GRATING PRESSURE SENSOR

Raman and Brillouin distributed temperature sensing are existing approaches for enhanced geothermal systems that have been used successfully for down hole temperature and strain measurements on a scale of a few tens of kilometers. These types of measurements will be included in the complete system. As part of this project, a quasi-distributed fiber Bragg grating (FBG) sensor is also being developed for multi-point pressure measurements in a geothermal system, making use of its multiplexing capability and small space requirements. Using a FBG sensor for geothermal pressure measurement has also recently been discussed in (Bremer, 2010).

When multiple FBGs are inscribed in a fiber, each one must have a unique grating period Λ_m. Multiple gratings construct a FBG array with reflected intensity peaks at $\lambda_1 = 2 \cdot n \cdot \Lambda_1$, $\lambda_2 = 2 \cdot n \cdot \Lambda_2$, …, $\lambda_k = 2 \cdot n \cdot \Lambda_k$. FBG sensors may be used in a strain-free package for distributed temperature sensing or thermal mapping along a geothermal well. An array of FBG sensors for which the packages are sensitive to pressure can be used as a distributed pressure sensor.

Although FBG temperature sensors have many advantages for use in geothermal wells, oil and gas reservoirs, bridges and structural health monitoring over other commercial temperature sensors such as thermocouples, IR cameras, thermistors, and RTD, the use of a conventional Type-I FBGs in sensors is limited to temperatures below 260 C. A metallized FBG sensor integrated within a metal package structure, however, can be used for pressure sensing up to 220 bars and temperatures up to 370 C.

Like Raman and Brillouin DTS sensing cables, FBG sensors must survive the harsh geothermal environment within a package suitable for a cable. However, when the fiber sensor is sealed in a package, the direct FBG pressure sensing capability is lost. Therefore, like the MEMS point pressure sensor package, the FBG package must integrate the FBG sensor and be functionalized to respond to the external geothermal well pressure variation. Since the temperature of a geothermal well may be up to 370 C, the corresponding thermal strain between the fiber sensor and metal package structure can reach a value of 2000-3000 $\mu\varepsilon$ (microstrain). A mechanical strain in the fiber is also produced by deformation of the package from the local well pressure. To distinguish between these two sources of strain, a differential method with one freestanding FBG sensor as a temperature sensor and another as both a

temperature and pressure sensor can make it possible to measure the local pressure in a geothermal well.

When adding a layer of metallization around a FBG, the thermal strain will be introduced by temperature, and the wavelength shift can be written as:

$$\Delta\lambda_B(t) = \lambda_B(1 - p_e)\left(\frac{Y_0}{1 + y}\right)(\alpha_m - \alpha_f)\Delta T$$
$$+ (1 - p_e)\varepsilon_m(t) + (\alpha_f + \beta_f)\Delta T \quad (1)$$
$$= \kappa_m \varepsilon_m(t) + (\kappa_t + \kappa_T)\Delta T$$

where $y \equiv \frac{Y_0 \cdot r_1^2}{Y_1 \cdot (r_2^2 - r_1^2)}$. $\alpha_f = 0.56 \times 10^{-6} \ C^{-1}$ is the thermal expansion coefficient of the fiber, α_m is the thermal expansion coefficient of the metallic coating, $\beta_f = 6.8 \times 10^{-6} \ C^{-1}$ is the thermo optic coefficient of the fiber, $\lambda_B \approx 1.53 \mu m$ and $p_e = 0.22$. κ_T and κ_t are the temperature and thermal strain sensitivity, respectively, of the FBG. Y_0 and Y_1 are Young's modulus of the fiber and metal coating, respectively. r_1 and r_2 are the radii of the fiber cladding and the metallized fiber, respectively. The structural mechanical strain induced in the FBG is a function of both pressure and temperature,

$$\varepsilon_m(P,T,t) \propto \Delta t(P,T,t)/L_o \quad (2)$$

where Δt is the pressure-induced axial mechanical deformation at the local temperature and pressure (T, P), and L_o is initial sensor package length. In a real geothermal well, the local temperature may vary slowly and the wavelength variation of the FBG peak is dominated by the pressure dynamics.
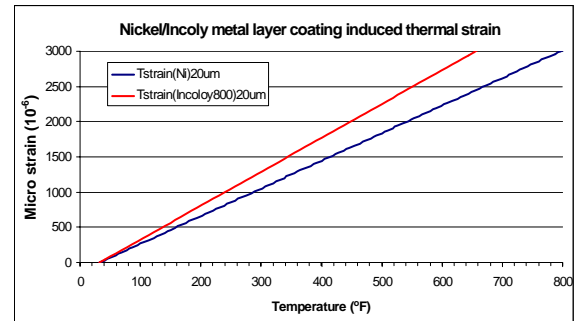

Fig. 4: *Metallized FBG as fiber strain sensor with nickel metallization*

In order to integrate a FBG with a package that can respond to the external pressure change, different bonding materials and metal coatings have been evaluated. The goal is to use a proper bonding material that can minimize the thermal strain between the fiber material and package structure, and enable the pressure-induced mechanical strain to be measured over a relatively large dynamic range. Fig. 4 is a simulation of thermal strain in a metallized

FBG sensor with a 20 μm nickel coating, and with an Incoloy800 coating. Both metal coatings exhibit about 3000 $\mu\varepsilon$ at 374 C (705°F). Although a linear model is used for the thermal strain estimation, the potential thermal strain from a 10-20 μm thick nickel layer may be ~2500 to ~4000 $\mu\varepsilon$ at the maximum operation temperature of 374 C.
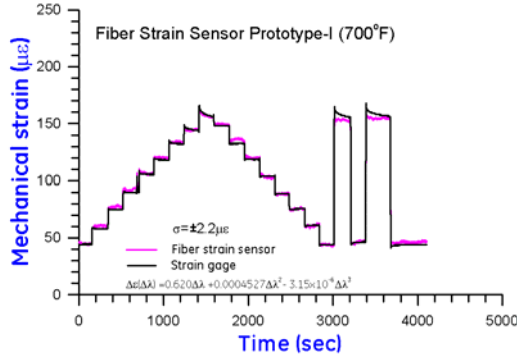
(a)
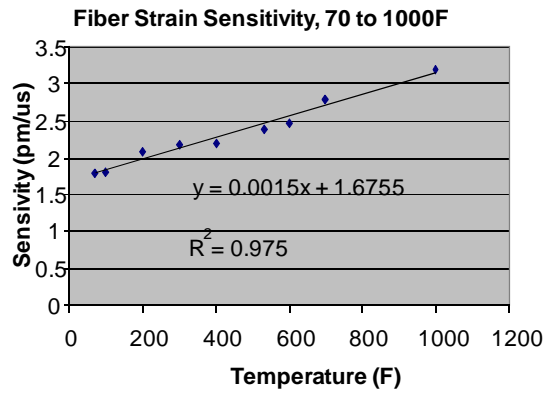
(b)

Fig. 5: (a) Strain response to a mechanical deformation by external force and (b) dependence of mechanical strain sensitivity on temperature for a prototype fiber strain sensor.

Fig. 5 is a comparison with a 10 μm nickel-coated FBG strain sensor where there is an electric resistive strain gage outside the oven for calibration and reference. The FBG sensor is bonded with a high-temperature adhesive material with a typical CTE of 10×10^{-6} C^{-1}, where the maximum bonding strength has been tested from 8000 $\mu\varepsilon$ to 12,000 $\mu\varepsilon$ at ambient temperature. At 371 C (700°F), the static strain test is consistent with a standard strain gage with a standard deviation of ±2.2 $\mu\varepsilon$. The transfer function of the fiber sensor's wavelength shift is normally given by a cubic polynomial function,

$$\Delta\varepsilon = a + b\Delta\lambda + c\Delta\lambda^2 + d\Delta\lambda^3, \qquad (3)$$

for temperatures greater than 260 C (500°F). On the other hand, when the temperature is less than 260 C, a linear transfer function works very well to convert mechanical strain into fiber sensor wavelength shift with a constant sensitivity of ~2 pm/$\mu\varepsilon$ as a first approximation. The measured mechanical strain sensitivity varies linearly with temperature, ~2.6 pm/$\mu\varepsilon$ at 260 C.

Fig. 6 demonstrates that two FBG sensors together can be used to measure both temperature and thermal strain. The FBG temperature sensor exhibits a sensitivity of ~5.76 pm/°F, but the FBG strain sensor has a thermal strain sensitivity of 12 to 16 pm/°F, depending upon the thicknesses of the metal coating and bonding materials. A metallized FBG is a temperature sensor if it is not fixed at both ends. When integrated with a package structure, however, a metallized FBG fixed at both ends can be designed to respond to both thermal and mechanical strains. The thermal and pressure-induced mechanical strains can then be separated by a differential calculation.

A 50 mm single-wall cylindrical mechanical package of stainless steel or Inconel surrounding a FBG fiber has been examined as a potential pressure transduction structure. This package should provide a mechanical strain from the expected external pressure variation that is comparable to the expected thermal strain. In addition, the total thermal and mechanical strain should be much less than the bonding strength of the bonding material or bonding method. However, the maximum pressure-induced mechanical strain is dependent upon the length, elastic modulus, and shape of the package material. The maximum bonding strength provided by a high-temperature adhesive material is 8000 $\mu\varepsilon$ to 12,000 $\mu\varepsilon$, so we restrict the total allowable strain for the package design to ~7000 $\mu\varepsilon$ to provide ~40% margin for maximum reliability. Fig. 7 shows the microstrain as a function of external pressure for a package we have designed from stainless steel. The fiber sensor is sealed inside the package by high-temperature adhesive material, and assuming the bonding material bond strength is greater than 7000 $\mu\varepsilon$. At 220 bar pressure, the transfer function of the pressure to mechanical strain is approximately 4383.8+10.908 *P(t)*, where *P(t)* is the pressure at a specific time. This transfer function is linear for pressures within ±10% of 220 bars. The thermal strain is ~4400 $\mu\varepsilon$, and the mechanical strain is ~2500 $\mu\varepsilon$, which is near the maximum range for the modeling calculation.
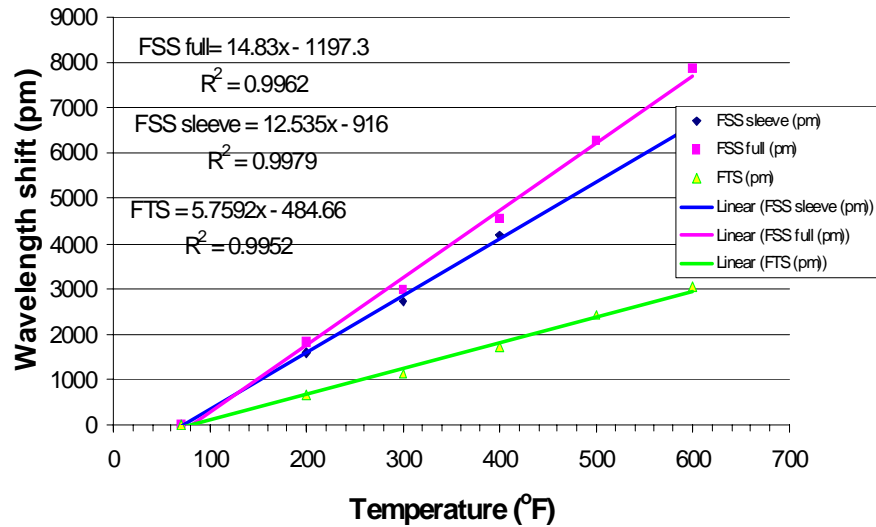
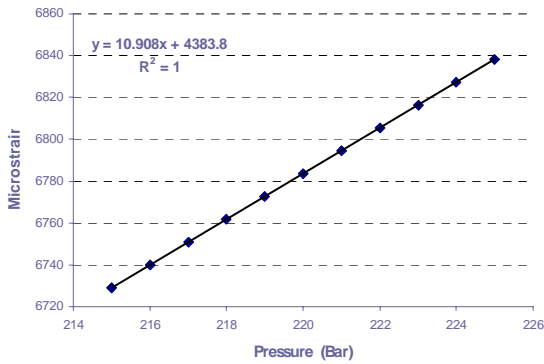Fig. 6: The measured temperature and thermal strain sensitivity for a fiber strain sensor.

Fig. 7: The fiber sensor mechanical strain response to pressure variation via package structure at 374 C (705°F).

FIBER OPTIC CABLE

As in the thermal recovery sector in Oil & Gas, EGS presents similar high temperature, hydrogen-rich well conditions that require high temperature, hydrogen tolerant optical fiber and low-strain cable designs to package the fiber in a low strain condition over repeated thermal cycles. The project team seeks to leverage such down hole oil and gas optical sensing cable designs and supply chain to meet the optical and mechanical requirements of the program to 300 C as a first temperature rating, intended to address the bulk of upcoming EGS resources, and 374 C to fully meet the requirements of the program.

A formal review of commercially available geophysical fibers was completed with both single mode and multimode fibers being evaluated, the latter specifically intended for Raman type distributed temperature sensors (DTS). Major fiber selection criterion includes use of pure silica core waveguide designs for resistance to hydrogen-induced attenuation, and high temperature fiber coatings including polyimide and metal coating

materials rated, respectively, to the two operating temperatures. Fiber suppliers considered include AFL/Fujikura Ltd., Corning Inc., Draka Communications, Fiberguide Industries, Fibertronix, IVG Fiber Ltd., Nufern, OFS Specialty Photonics, Sumitomo Electric Industries, and Verrillon.

Table 1: Fibers selected for mechanical strength testing at high temperatures

Waveguide	Coating	Rating
50/125 MM Step-Index Pure Silica Core	Polyimide	300°C
50/125 MM Graded-Index Control	Polyimide	300°C
50/125 MM Step-Index Pure Silica Core	Polyimide	300°C
50/125 MM Graded-Index Synthetic Silica	Polyimide	300°C
9/125 SM Step-Index Synthetic Silica	Polyimide	300°C
9/125 SM Step-Index Pure Silica Core	Polyimide	300°C
9/125 SM Step-Index Pure Silica Core	Polyimide	300°C
9/125 SM Step-Index Pure Silica Core	Polyimide	300°C
50/125 MM Step-Index Pure Silica Core	Aluminum	400°C
100/140 MM Step-Index Pure Silica Core	Aluminum	400°C

A fiber test and evaluation program has been implemented that characterizes both fiber mechanical and optical performance for a set of ten candidate fibers listed in Table 1 that was procured commercially. Mechanical performance assessment is based on dynamic tensile testing and Weibull statistical analysis to generate reliability models used in the telecommunications fiber industry.
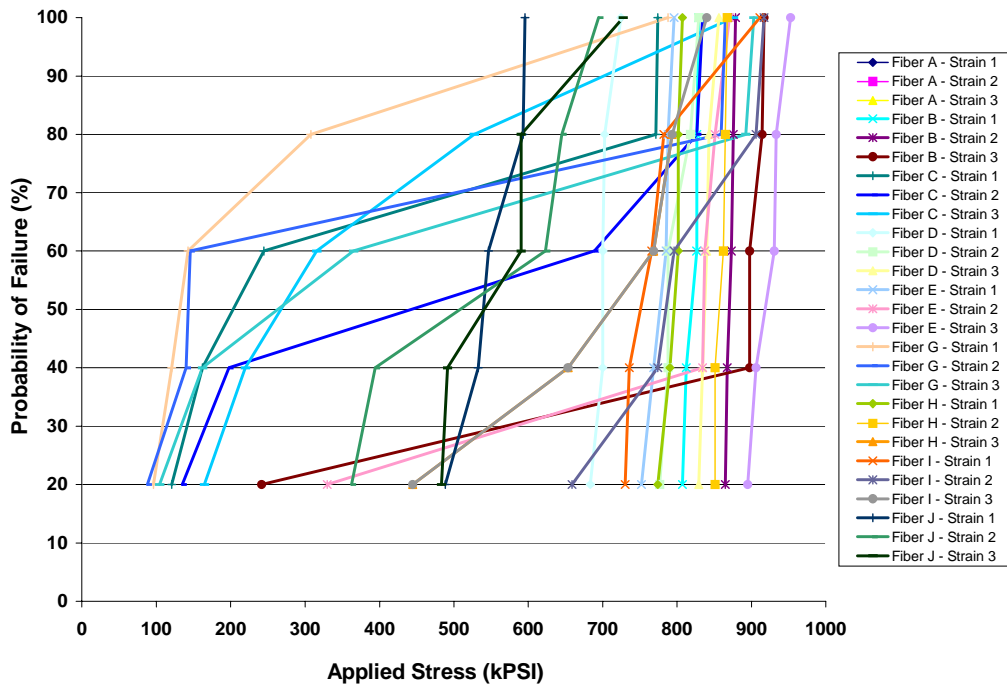
Fig. 8: Fiber dynamic test results for as-received fiber.

This analysis starts with fibers as procured, followed by sets of fiber conditioned at temperature to characterize any aging and degradation of fiber inherent mechanical strength from thermal conditioning. Baseline as-received fiber dynamic strength results in Fig. 8 show a large Weibull distribution, with some fibers exhibiting poormechanical performance even before thermal conditioning. Results after three thermal conditioning periods up to 500 hours likewise are varied, with four fibers demonstrating encouraging Weibull statistics under aging as seen in Fig. 9 for one of the polyimide-coated single mode fibers.

Optical performance characterization of the fibers includes baseline optical performance properties as applied to the sensing application, for example as a transmission fiber or sensing fiber, and reactive, i.e., permanent hydrogen-induced attenuation at prescribed temperature and hydrogen partial pressure atmospheric conditions. Hydrogen tests are being performed using a pressure vessel and pure hydrogen at elevated temperature. The hydrogen test apparatus includes high pressure optical penetrators to allow continuous monitoring of fiber attenuation at multiple wavelengths including 850 nm, 1310 nm, and 1550 nm. For multimode fibers intended to operate Raman DTS systems, a DTS interrogator is used to monitor temperature offset and attenuation at pump and backscattered Stokes/anti-Stokes wavelengths.

At the conclusion of this activity, a set of both single mode and multimode fibers will be qualified for use in high temperature EGS cables. This cable design will be based on current down hole oilfield cables, with design features specific to the well conditions and uncased wellbores of EGS.

CONCLUSION

An overview and some of the details of a project for developing a fiber optic cable to measure down hole pressure and temperature in enhanced geothermal systems has been described. A highly accurate point pressure measurement at the bottom of the well will be accomplished by a MEMS pressure sensor. Distributed temperature and pressure measurements will be obtained by FBG sensors. Other techniques such as Raman DTS, Brillouin DTSS and Rayleigh COTDR will be employed if robust fibers that resist hydrogen darkening at the high temperatures and pressures of geothermal wells can be obtained. Initial results from optical measurements on existing low pressure MEMS sensors indicate that adequate SNR is possible for the point pressure measurement even with some light loss over a 10 km fiber length. A MEMS sensor has been designed for operation with a single fiber for delivering the drive and readback laser beams, and is being fabricated.
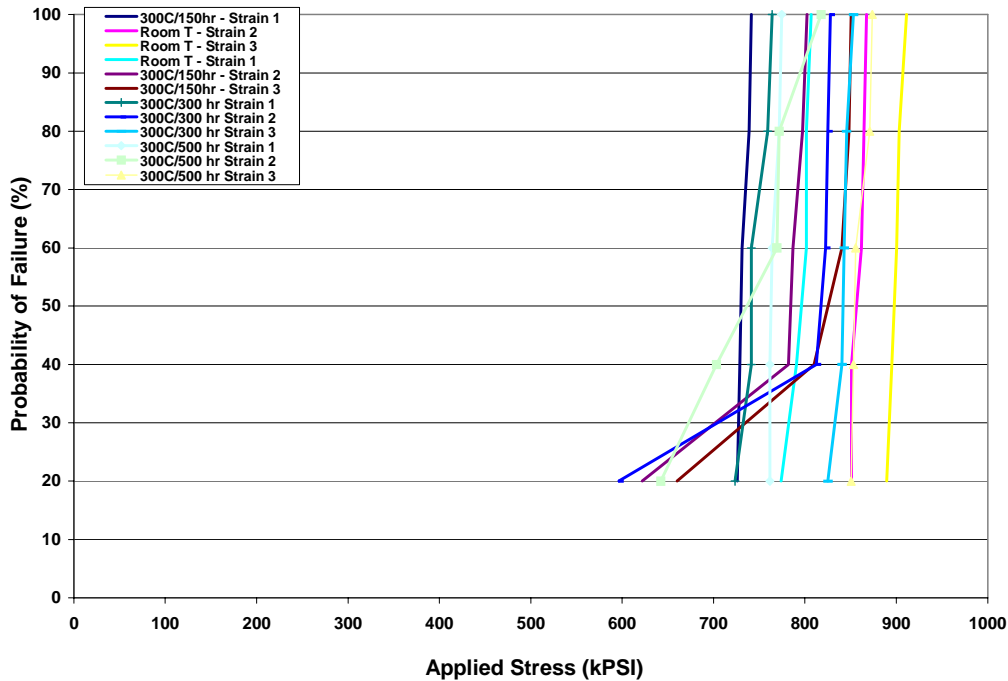
Fig. 9: Fiber dynamic test results after thermal conditioning

A fiber Bragg grating pressure sensor for distributed geothermal wells using wavelength-multiplexing has been described. A package has been designed with an integrated metallized FBG fiber sensor. The fiber sensor is to be bonded into the package to respond to the external pressure dynamics by mechanical strain detection. A second FBG sensor that is not sensitive to pressure can be sealed into the same package and used to deconvolve the pressure effect from the temperature effect of the first sensor. For reliable operation, the mechanical and thermal strains should be much less than that of bond strength provided by the bonding material.

ACKNOWLEDGEMENTS AND DISCLAIMER

REFERENCES

Andres, M. V., Foulds, K. W. H., Tudor, M. J. (1986) "Optical activation of a silicon vibrating sensor," *Electron. Lett.* **22** (1986) 1097-1099.

Bremer, K., Lewis, E. Leen, G., Moss, B., Lochmann, S., Mueller, I., Reinsch, T., and Schroetter, J. (2010) "Fiber optic pressure and temperature sensor for geothermal wells," *IEEE Sensor Conf.* 538-541.